Analysing the effects of local environment on the source-sink balance of Cecropia sciadophylla: a methodological approach based on model inversion

Veronique Letort, Patrick Heuret, Paul Camilo Zalamea, P. de Reffye, Eric A. Nicolini

Analysing the effects of local environment on the source-sink balance of *Cecropia sciadophylla*: a new methodology based on model inversion.

Véronique LETORT*, Patrick HEURET, Paul-Camilo ZALAMEA, Philippe DE REFFYE, Eric NICOLINI

Institutions where the study was performed:

MAS, Ecole Centrale Paris, Chatenay-Malabry, F-92290 France

INRIA Futurs, EPI Digiplante, Orsay, France

INRA, UMR AMAP, Montpellier, F-34000 France

IRD, UMR AMAP, Montpellier, F-34000 France

CIRAD, UMR AMAP, Montpellier, F-34000 France

Universidad los Andes, Departemento de Ciencias Biologicas, Bogota, Colombia

* Corresponding author :

Ecole Centrale Paris - Laboratoire MAS - Grande Voie des Vignes – F-92295 Châtenay-Malabry cedex - FRANCE

Phone: +33 (0)141131765 Fax: +33 (0)141131735

veronique.letort@centraliens.net

Short title: A functional-structural model for *Cecropia*

Key-words : *Cecropia* / functional-structural model / model inversion / morphology / trophic competition

Total number of characters: 35165

Number of Figures: 7 ; Number of Tables: 2

Abstract:

- Functional-structural model (FSM) of tree growth have great potentials for the forestry field but their development, calibration and validation are hampled by the difficulty to collect experimental data at organ scale for adult trees. Owing to their simple architecture and morphological properties, 'model plants' such as *Cecropia sciadophylla* are of great interest to validate new models and methodologies since exhaustive descriptions of the plant structure and mass partitioning are accessible.
- The objective of this study was to propose a methodology and to analyse the influence of environmental conditions on the dynamics of trophic competition within the trees.
- Using data of 11 trees measured in September 2007 for calibration and data of 7 trees measured in December 2008 for validation, we present a method to estimate an integrated factor of local environment for each plant, based on model inversion of the GreenLab FSM. It provides as a result the complex dynamics of biomass allocation to the different components of the plants during their growth, according to the environmental pressure they underwent.
- Extension of the model to population level could be done by linking the integrated environment factor to a competition index.

Introduction

Classically, individual-based forestry models use simplified representations of tree crown and characterize the growth by variations of key indicators such as height or diameter at breast height (Pretzsch, 2002). In the last decades, a new class of plant growth models has emerged, representing trees at organ scale and integrating structural and functional processes, and their interactions with the environment (Sievänen et al., 2000; Prusinkiewicz, 2004). However, their potential application to the field of forest management is not straightforward. A major obstacle is model calibration and validation against adequate data. For adult trees, their high stature, complex structure, and long life span drastically increase the experimental work required to collect data at organ scale. So, practically, only global, aggregated or sampled measurements are used to develop and evaluate the models (e.g. in Perttunen et al., 2001; Lopez et al., 2008).

In that context, another promising approach is to consider 'model trees' with a reduced lifespan and structure complexity to build and validate FSTM. The neotropical genus *Cecropia* Loefl. is the most important genus of pioneer trees in the neotropics; it grows rapidly and ably colonizes gaps (Berg and Rosselli, 2005). It includes 61 species that possess several properties of a 'model tree'. *Cecropia* has a very simple architecture following a Rauh model (Hallé et al., 1978). Each node bears three lateral buds that potentially give rise to a branch (central bud) and two inflorescences (Zalamea et al., 2008), as illustrated in Fig. 1B. Branching

and flowering are immediate; growth is continuous (no period of cessation of growth). The number of phytomers constituting the whole tree remains relatively low even though the life span can reach several decades. In previous studies, Heuret et al. (2002) and Zalamea et al. (2008) have shown a high annual periodicity in reproductive and branching processes, as well as an alternation of long and short nodes, for *C. obtusa* and *C. sciadophylla* respectively. Additionally, their results indicate that it is possible to estimate the age of a tree by observing its morphology, due to the fact that stipules, leaves, inflorescences, and branches scares remain visible along growth axes.. This is especially interesting in these tropical zones where tree age determination is difficult.

The origins of these periodic patterns might be linked, among others, to climatic fluctuations and/or dynamic trophic competition during the plant development. The question is thus: how to analyse the effect of environment on source-sink balance?

Unravelling the environment influence from the trophic dynamics can be done using a FSTM. But determining how to define the environment factor to input in the model is complex since many factors interact together and are impossible to measure with accuracy. Therefore, in our approach, we chose to characterize the environment by a single variable, that would represent the integration of every environmental factors and would be an indicator of the plant potentiality at each growth step. For suitable models, this integrated environmental factor can be

89 estimated together with the model parameters using tree data.

90 In this study, we present the application of that method, using inversion of the
91 FSTM GreenLab (Yan et al., 2004; Mathieu et al., 2009), for analysing the
92 environmental influence on the source-sink balance for *Cecropia sciadophylla*. A
93 previous study of *Cecropia* using the GreenLab model was performed in Letort et
94 al. (2009) using data of 11 trees that were measured in French Guiana in
95 September 2007. However, the environment was considered as a constant factor. It
96 did not allow to analyse the influence of the seasonal fluctuations of the Guyanese
97 climate (alternation of dry and rain seasons) on plant growth. Especially internode
98 lengths seem to be related to rainfall (Heuret et al., 2002; Zalamea et al., 2008). A
99 new methodology had to be introduced and the model had to be adapted to take
100 into account the intra-annual variations of the environmental pressure. Besides, a
101 new set of data on seven trees was collected in December 2008 and was used as an
102 independent dataset for validation of the method.

103

104 With the objective of using the model as a tool to unravel the ontogenic variations
105 (low-frequency trend) and the environmental variations (high-frequency
106 variation), the aims of this work are (i) to determine morphological allometries to
107 simplify future measurements, (ii) to evaluate the ability of the GreenLab model
108 to trace back the dynamics of internal trophic competition within the plants, and
109 (iii) to evaluate the possibility of driving the morphological and architectural
110 plasticity by a single control variable. Eventually this study paves the way to the

111 definition of an index of competition, in order to obtain a forest model based on
112 individual trees with explicit architectures and to analyse the emergent properties
113 at stand level.
114
115 **Materials and methods**
116
117 The individuals sampled for this study were taken from two sites in French
118 Guiana: Saint-Elie road (5°17'N, 53°04'W) and Counami road (5°24'N, 53°11'W).
119
120 *Measures and experimental protocol*
121
122 In September 2007, 11 individuals were felled and measured, ten at Saint-Elie
123 road and one at Counami Road. All the trees from Saint-Elie population were
124 sterile and only one had branches. The tree from Counami road was pistillate and
125 had branches.
126 In December 2008, dataset was completed with seven individuals measured at
127 Counami Road. They were all sterile and without branches.
128
129 Trees were described node by node following the protocol defined by Heuret et al.
130 (2002). Tree topology, *i.e.* the relative position nodes and axes, was recorded
131 following the MTG formalism (Godin and Caraglio, 1998) and analysed using the
132 Vplant package, the successor of AMAPmod (Godin et al., 1997) now integrated

133 in the OpenAlea platform (Pradal et al., 2009). The age determination of trees and
134 annual growth delimitation were performed following the protocol proposed by
135 Zalamea et al. (2008). For each phytomer, the following information was
136 recorded: the length of the underlying internode, the diameter in the middle of the
137 internode, and the presence of developed branches, inflorescences and/or leaves at
138 each internode. The blade was weighed. For trees of 2007, blades were pressed
139 between two plates of Plexiglas and then photographed using a digital camera
140 with a focal length of 50 mm. Blade areas were estimated by analysing the
141 photographs with the ImageJ freeware (http://rsbweb.nih.gov/ij/). The length, the
142 diameter in the middle and the fresh weight of the petioles were recorded.
143 Inflorescence or infructescence were weighted. The plant axes were then cut node
144 by node, 1 cm above the top of the stipule scar. The length of the cut segment (not
145 exactly equal to the internode as there is a 1 cm shift) was recorded as well as its
146 fresh weight and two orthogonal diameters of the pith. Internodes, leaves,
147 infloresences, and petioles were dried at 103°C during 72 h and the dry mass was
148 measured. For young individuals, the root system was extracted, washed, dried
149 and weighed.
150
151 *Model of biomass production in GreenLab for Cecropia*
152
153 GreenLab is a dynamic model of plant growth that aims at simulating plant
154 topological development, biomass production and allocation at organ scale. For

155 sake of simplicity, we use here the discrete version of GreenLab, where the
156 simulation step is based on the rhythm of plant development both for the
157 organogenesis part and for the functional part of the model. This simulation step is
158 set as the duration between emission of two successive phytomers along the main
159 axis and is called the Growth Cycle (GC). For *Cecropia* species, after some
160 variability during the phase of growth establishment, the rate of emission of new
161 phytomers is remarkably stable (Heuret et al., 2002): each axis increases by 2-3
162 nodes per month for *Cecropia sciadophylla* (Zalamea et al., 2008).
163
164 At plant emergence, the initial biomass is provided by the seed, *Q(0)*. The,
165 biomass production at every GC is set to be simply proportional to blade area *S(t)*,
166 multiplied by a factor that represent the environmental pressure, *E(t)* :
167 $$Q(t)=\mu \cdot E(t) \cdot S(t) \qquad (1)$$
168 where μ can be seen as a coefficient of conversion of a given environmental input
169 *E* into biomass. No self-shading is taken into account in this equation, given the
170 particular arrangement of leaves: they are located at tips of branches with
171 phyllotaxy 5/13. Low self-shading was also reported by Kitajima et al. (2002) for
172 *Cecropia longipes*. The environmental factor *E(t)* is defined in the next section.
173
174 *The environmental factor*
175
176 We decompose the environment factor into two parts: one with temporal

177 variations that corresponds to the climatic variations and is thus common to every
178 plant of the same region; the other one is a constant relative site local index,
179 defined on an arbitrary scale, which is a multiplicative factor that set the relative
180 level of local conditions on each site compare to each others, thus accounting for
181 local spatial variations. This integrated index might aggregate the levels various
182 local factors such as soil quality, nutriment and water availability, local density,
183 etc.
184 Climate in French Guiana is seasonal with a 3-months dry season from mid-
185 August to mid-November and a rain season during the other 9 months.
186 Additionally, a short dry season may occur in February and March.
187 A new function was added in the model to represent these seasonal variations of
188 precipitations over an average year. The absolute value of a sinusoidal function
189 was chosen, and truncated by a constant threshold B to set the duration of the dry
190 season. The environmental factor integrated over month i ($0 \leq i < T$ with the
191 origin $i=0$ in October at the middle dry season) for an average year is then defined
192 as follows:

193 $$e_i = m_i \cdot Max\left\{B, \left|A \cdot \sin\left(\frac{i \cdot \pi}{T}\right)\right|\right\} \quad (2)$$

194 where T=12 is the period (one year), A is the amplitude of the variations of
195 precipitations that will be fitted to the precipitation data, B the truncation
196 threshold: it corresponds to the average amount of precipitations during the dry
197 season. The short dry season was included in the climate function using a

198 multiplicative factor, m_j ($0 \le m_j \le 1$), which is equal to $1\text{-}a$ ($0 \le a \le 1$) during the
199 month m of the short summer season, and is equal to 1 otherwise.
200
201 The parameters B, A, a and m were estimated using the precipitation data of the St
202 Elie meteorological station from 1978 to 1991 (Fig. 2).
203
204 To use this function as control variable for the growth of *Cecropia* trees, we need a
205 change of variable from the calendar time to GC. A preliminary step is thus to
206 input the number of phytomers, T_y, emitted every year for each plant. Then, for a
207 given individual I, the environmental factor integrated over GC j of year y can be
208 defined as:

209 $$E^I_{j,y} = E^I \cdot m_{j,y} \cdot \frac{T}{T^I_y} \cdot Max\left(B, \left|A \cdot \sin\left(\frac{j \cdot \pi}{T^I_y} + \varphi^I_0\right)\right|\right) \qquad (3)$$

210 where the index I denotes the variables that are specific to each individual: E^I is
211 the relative local index; φ^I_0 is the phase at origin: it depends on the time when the
212 plant I emerged from the seed; T^I_y is given for every plant I and each year y, based
213 on the annual growth delimitations recorded. The ratio T/T_y comes from the
214 change of variable and corresponds to a normalization the total amount of
215 precipitation received by each plant over the year.
216 The short dry season is modelled by:

217 $$m_{j,y} = \begin{cases} 1-a & if \ \frac{m T^I_y}{T} \le j < \frac{(m+1) T^I_y}{T} \\ 1 & else \end{cases} \qquad (4)$$

This equation is valid if φ_0=0 and a simple translation of phase is performed otherwise.

Model of biomass allocation

The allocation process is modelled with two steps: first, biomass is allocated to the four compartments of plant growth: primary growth of phytomers, biomass for ring increment (secondary growth), expansion of inflorescences, roots, then there is intra-compartment partitioning to each organ.

The root mass of young individuals allowed us to build a simple allometric relationship for the biomass allocated to the root system at each GC: it is simply set proportional to the biomass production. The remaining biomass, $Q_r(t)$, is partitioned between the three other compartments in proportion to their respective demands, $D_c(t)$, where c stands for primary growth (*pg*), inflorescences (*inflo*) and ring increment (*ring*) respectively. So, $D(t)$ being the plant total demand at GC t, *i.e.* the sum of the demands of the three compartments, the amount of biomass that goes to compartment c is:

$$Q_c(t) = D_c(t) \cdot \frac{Q_r}{D}(t) \quad (5)$$

$$\text{with} \begin{cases} c = pg: & D_{pg}(t) = \sum_{Buds(t)} P_b \left(1 - e^{-K_b(o)\cdot k}\right) \\ c = inflo: & D_{inflo}(t,n) = \sum_{Inflos(t)} P_{fl} \cdot \varphi(n; a_{fl}, b_{fl}, T_{fl}) \\ c = ring: & D_{ring}(t) = P_{rg} \cdot L(t) + K_{rg} \cdot \frac{Q}{D}(t) \end{cases}$$

where the demand for primary growth $D_{pg}(t)$ is the sum of the demands of every active meristem (noted "Buds" in the equations), designed by its rank k and branching order o. Letort et al. (2009) have shown the existence of a transitory phase when meristems are young (at axis emergence). The duration of that transitory phase is driven by the parameter $K_b(o)$, that depends on the branching order o. Afterwards, meristems reach a stable phase where they all have similar sink P_b whatever their rank and branching order. Sink parameter P_b is taken as reference for the other compartment demands so its value can be arbitrarily set.

The demand of inflorescences $D_{inflo}(t)$ is defined as the sum of the sink strength of every growing inflorescence of the plant at GC t. The sink strength is P_{fl} and its variations with inflorescence age n follow a beta law density function whose parameters are a_{fl} , b_{fl} , and the expansion duration T_{fl} (see Yin et al. (2003) and Christophe et al. (2008) for expression and use of beta law density function).

The demand for ring increment is assumed to consist of two parts: the first one is proportional to the total length of all axes of the plant. The sink linear density is P_{rg}. The second one is proportional to the ratio of biomass supply to demand, Q/D. It implies that vigorous plants invests relatively more in their ring compartments, compared to plant that are stressed and have thus a low Q/D value.

The intra-compartment partitioning is straightforward for the compartments of primary growth and inflorescence growth: each component receives an amount of biomass proportional to its demand. Then, inside each bud, biomass is partitioned

between blade, petiol and internode using allometric proportions p_b, p_p, and p_i: indeed, data analysis revealed a good proportionality between organ mass and phytomer mass (see Results part). The partitioning of ring biomass to each phytomer follows the principles similar to those of the Pipe model of Shinozaki et al. (1964): each internodes receive an amount of biomass proportional to its length and to the total area of blades localized above it in the tree architecture (see Letort et al. (2008) for further details).

Allometric relationships link organ volume and its geometrical dimensions. Internode length is calculated from internode volume by assuming a cylinder shape:

$$l = Be \cdot V^{\beta} \qquad (6)$$

Blade area is calculated from blade mass by:

$$S = \frac{M}{SBM} \qquad (7)$$

where *SBM* is the specific blade mass (g.cm^{-2}). The parameters *Be* and *SBM* are of special interest for Cecropia since they have a strong influence on the source-sink balance: internode length determines ring demand; blade area determines the plant production. It was also observed that they vary with time and among different individuals. Therefore a mechanistic modelling was the objective: these allometries were set dependent on the source-sink balance of each plant.

Classically, the ratio of biomass supply to demand, Q/D, is taken as a key variable

of the GreenLab model and is considered as an index of the level of internal trophic competition (Mathieu et al., 2009). Here, the variations of Q/D are from two sources: the high frequency variations represent the response of the plant to seasonal environmental stress while the low-frequency variations represent the global trend of trophic competition. Since it seems not realistic to have so fast variations of these allometries, we extract this low-frequency trend: we define the variable $A_T(Q/D(t))$ which is the average of the Q/D values over the previous year. So the following equations were chosen:

(1) $$Be(t,k) = Be_{min} + Be_{max} \cdot \exp\left(-K_{Be} \cdot k \cdot A_T(Q/D(t))\right) \quad (8)$$

at GC t and rank k, where Be_{min}, Be_{max} and K_{Be} are parameters to estimate.

(2) $$SBM(t) = Min\left\{SBM_{max}, SBM_{min} + K_{SBM} \cdot A_T(Q/D(t))\right\} \quad (9)$$

where SBM_{max} is the SBM at measurement date, input for each tree, SBM_{min} is the minimal observed value and K_{SBM} is a parameter to estimate.

Additionally, leaf functioning duration was also set as an affine function of $A_T(Q/D)$. It was indeed observed that the number of active leaves varied with tree development and environmental conditions. A leaf appearing at GC t will stay photosynthetically active during T_a GC:

$$T_a(t) = T_{a,min} + K_a \cdot A_T(Q/D(t)) \quad (10)$$

where $T_{a,min}$ is the minimal value that was observed and K_a is a parameter to estimate.

302 *Parameter identification of the model*

303

304 Some allometric relationships were first estimated directly from the data, using the
305 R software (R Development Core Team (2008)). In particular, we used the data
306 from 2007 to derive a model for a faithful prediction of blade area using petiol
307 fresh sectional area. Indeed, large blades produces more biomass that needs to be
308 exported to the rest of the plant and thus necessitate a large sectional area of the
309 corresponding petiol. Another advantage is that is very easy to measure. The
310 allometry was then applied to estimate blade areas for the 2008 data.
311 Then target files were filled with the data of tree topology (position of branches
312 and inflorescences), and data of organ mass and dimensions of the 11 trees of the
313 2007 and 2008 protocols: internode dry mass, length, diameter; blade dry mass
314 and area; petiol dry mass; inflorescence dry mass, for each phytomer. Additionally,
315 a file giving the number of phytomers emitted per year was input for each plant.
316 The shape of environmental variations was set using the parameters estimated on
317 the precipitation data. The estimation of the relative local index for each plant site
318 and of the remaining hidden parameters was performed using the *Digiplant*
319 software (Cournède et al., 2006). An adaptation of the 2-stage Aitken estimator
320 was used, where the observations are classified into groups with respect to the
321 type of organs (that have potentially very different size orders) and the error term
322 of each group has common unknown variance and errors are mutually independent
323 (Zhan et al., 2003; Cournède et al., 2011). Only the data from 2007 protocol were

used for estimating the model parameters. Then data from 2008 protocol were used for validation, only estimating their relative local index of environment.

Results

Data analysis

Fig. 1C-D shows two of the measured individuals (ID 4 and 10). Tab. 1 presents some characteristics of the measured trees. The oldest measured trees are 8 year-old and had approx. 230 phytomers on the main stem. There is a large inter-tree variability: for instance, Tree 9 is five years younger than Tree 8 but is nearly as large (approx. 40 kg). For trees 1, 2, and 30, that all have between 50 and 55 phytomers, aerial mass varies from 0.2 to 5.5 kg.

Root dry mass was measured for the eight youngest individuals of 2007 measurements. The ratio between root mass and total mass was found of 0.19 in average (s.d. 0.059).

Tree age results from the procedure of year delimitation based on the sequence analysis of organ dimensions along the main stem, and based on the position of branches and inflorescences when they were present (Fig. 3).

The allometry relationship between blade area (cm^2) and petiol sectional area

346 (mm^2) was obtained using n=523 data points, giving a coefficient of 35.18
347 (R^2=0.975; Fig. 4A). More precisely, a key variable of our model is the SBM
348 (blade dry mass/ blade area): Fig. 4B shows the comparison between SBM
349 calculated from measured or estimated blade areas. The results are satisfying
350 except for low values of petiol section.
351
352 For intra-phytomer partitioning of biomass, observations of young phytomers
353 (n=540 leafy phytomers) suggested a linear model of organ dry mass with respect
354 to phytomer dry mass. To be biologically realistic, it was imposed that organ mass
355 is zero when phytomer mass is zero. Fig. 5 and Tab. 2 present the results for
356 blades ($y = 0.7177 \cdot x$, R^2=0.99), petiols ($y = 0.2080 \cdot x$, R^2=0.97) and internodes
357 ($y = 0.07423 \cdot x$, R^2=0.81). Note that Individual 9 was not included (although
358 represented on the graphs) since its high values of internode mass let suspect that
359 secondary growth might not be negligible for this individual even on young
360 phytomers.
361
362 *The environmental factor, representing precipitations at St Elie station.*
363
364 Analysis of our precipitation data showed that the so-called "short summer of
365 March" was more likely found in February (m=4 in Eq. (4)). The parameters
366 estimated for the environmental fluctuations over an average year are given in Tab
367 2. The comparison between recorded and fitted data is presented in Fig. 2.

368

369 *Fitting results.*

370

371 Tab. 2 gathers the values of the parameters used in the simulations. The values of
372 the model hidden parameters and individual local environment indices were
373 estimated using the 11 individuals of 2007 protocol. Fitting in parallel their data of
374 organ dimensions and mass represented in total more than 4600 data points, while
375 the number of degrees of freedom (number of parameters to identify in parallel)
376 was 24. Some parameters were fixed, based on observations and biological
377 knowledge: the initial biomass, coming from the seed, was set to 0.1g; the
378 parameter β defining internode shape was set to 0.9 since internode length was
379 highly variable; duration of inflorescence expansion was observed to last
380 approximately 7 GC; the initial value of leaf functioning duration was set to 7
381 according to the minimal number of active leaves observed on young plants;
382 primary growth compartment (buds) was chosen as the reference for the model of
383 proportional sinks and could be set arbitrarily: the value 10 was chosen. It is
384 interesting to note that the ratio between the sink bud parameters $K_b(1)$ and $K_b(2)$
385 is 1.04, which means that the demand of the apical meristem of branches follows
386 nearly the same trajectory as that of the main stem. The parameters P_{rg} and K_{rg} are
387 close but the resulting ring demand consists in fact at approximatively 90% of the
388 part of the demand which depends on the total axis length (linear density of sink
389 for rings).

390

391 Fig. 6 presents some of the fitting graphs: measured and simulated values of
392 internode mass (a), blade mass (b), petiol mass (c) and inflorescence mass (d) for
393 the main stems of the 11 individuals. The sinusoidal variations of internode mass
394 are generated by the environmental fluctuations. Although the fitting accuracy
395 looks correct at visual inspection, the coefficient of determination are relatively
396 low (0.43, 0.79, 0.43, 0.45, 0.50 for internode mass, diameter, blade mass, blade
397 area, and petiol mass respectively) because of the sinusoidal shape of these curves.
398 The coefficients of determination for the cumulated values (internode, blade and
399 petiol compartments) are all above 0.98.
400 The validation with data from 2008 are acceptable: coefficients of determination
401 are 0.43, 0.75, 0.07, and 0.18 for the same variables. The inaccuracy on blade and
402 petiol mass is due to some variability in the number of active leaves that are
403 present. For cumulated values, the coefficient of determination are also all above
404 0.98.
405 Although not perfect, these fittings prove that it is possible to reproduce the large
406 variability that was observed for our target trees with a common model where the
407 environmental pressure is integrated into a single factor.
408

409 The variations of the biomass supply to demand ratio *Q/D* are presented in Fig.
410 7(A). The strong fluctuations are related to the seasonal variations of the
411 environment. Fig. 7(B) shows the global trend of *Q/D*: its values were averaged

412 over one year. A strong increase was observed after the appearance of the first tier
413 of branches for tree 8 and tree 10. In contrast, the growth inflorescences decreased
414 the *Q/D* ratio, as expected.
415
416 **Discussion**
417
418 The relative simplicity of *Cecropia* architecture made it possible to analyse the
419 growth of the tree with the GreenLab model, using a complete description at the
420 same scale as the simulation scale. It even offered the possibility to include in total
421 18 plants in the analysis. The advantage of multi-fitting (fitting several plants in
422 parallel) have been demonstrated for crops with GreenLab (Guo et al. 2006) and is
423 even more crucial for trees given their high variability. By fitting several plants in
424 parallel, we expect to extract a set of stable parameters that would be
425 representative of the species, and to avoid that the fitting would be too much
426 perturbed by individual random particularities of single plants (known as problem
427 of over-optimisation). Additionally, it allows testing the robustness of the model
428 and its ability to simulate several plants with the same parameter values, with only
429 one site-specific factor to explain the observed variability.
430
431 Simulations using the parameter values estimated in this multi-fitting process
432 provides the dynamics of the different compartment biomass and of the ratio of
433 biomass supply to demand for each plant. No obvious conclusion can be drawn

434 concerning the link between this ratio and the appearance of the first tiers of
435 branches and inflorescences. Nevertheless, it shows that tree 8 has a ratio of
436 biomass supply to demand, *Q/D*, a bit lower than that of tree 10, which might
437 explain its later emission of branches. But given that tree 9 had a very high *Q/D*
438 ratio but no branches, it is likely that other factors than the trophic competition are
439 involved in the appearance of branches. From Fig. 7, it seems that branches
440 contribute greatly to the plant production and are more sources than sinks. The
441 interpretation of Fig. 7 suggests new hypotheses for the senescence of *Cecropia*:
442 when an axis grows in height, its production tends to reach a saturation level while
443 its demand increases regularly because of the increasing load of rings. If no
444 branches appear, this would end to the death of the plant.
445
446 However, this behaviour is strongly linked to the modelling choices, as illustrated
447 by the comparison with the curves found in Letort et al. (2009), that were obtained
448 with a constant environment and a less mechanistic model. In particular, several
449 weaknesses of the current model can be highlighted. Two variables are still input
450 directly in the simulation instead of being modelled: the maximal value for the
451 specific blade mass and the number of phytomers emitted per year. The latter is all
452 the more important when considering the annual environmental variations, since a
453 difference of phase would perturb the fitting results. But questions remains on
454 what factors affect the organogenesis rhythm and it is likely that strong random
455 effects induce the variability observed during the first years after plant emergence.

A second question that arise from this work is the possible existence of interactions between the plant structure and its strategy for biomass allocation. First, the presence of stilt-roots has been observed on some individuals, but were considered as part of the root system in this study. But, given the particular candelabrum-like architecture of *Cecropia* and the important heights that they can rapidly reach, a natural hypothesis would be that the appearance of stilt-roots, as well as the demand of the ring compartment, could be influenced by requirements to ensure the mechanical stability of the tree. Such hypothesis could be investigated in parallel by an experimental approach and by a model-based approach: indeed, since the calibrated model faithfully reproduce internode masses and dimensions along the main stem, it would be possible to calculate the biomechanical stresses in the trunk at each growth step, as done by Qi et al. (2009) with the GreenLab model for a virtual tree. Thus, virtual experiments could be performed to understand the potential relationship between ring increment or stilt-root growth and the mechanical stability of the tree.

A result of our study was the introduction of an environmental factor that consisted of two parts: one for the temporal variations, related to the amount of precipitations over an average year; and the other one, constant through time and set for each individual, that corresponds to the global level of environmental pressure on the plant, as the integration of many different factors. This might look like an oversimplification, in contrast with most FSTM that integrate the effects of

many environmental factors (PAR, water, nitrogen content, etc) on the plant growth at fine scales (e.g. Lopez et al. (3008)). But in natural conditions, it is difficult to characterize the environment of each plant in details because of the numerous local heterogeneities and to unravel the respective influences of the different factors. The choice of a single, integrative factor might then be considered and in our study, the large inter-plant variability of the data was successfully reproduced. The interest of a model where tree growth and, potentially, architecture (see Mathieu et al., 2009) are driven by a single environmental factor, is that it paves the way to extension from individual-based model to population level (Cournède et al. 2008). Indeed, this simple environmental factor could be related to an index of competition to simulate the growth of a stand.

Acknowledgments

The authors thank the students who helped us for the measurements during the training programm FTH organized by AgroParisTech, Kourou (UMR Ecofog): V. Bellassin, S. Braun, O. Djiwa, V. Le Tellier (FTH2007), L. Menard, A. Jaecque, K. Amine, J. Kaushalendra (FTH2008). We also thank B. Leudet, J. Beauchêne and F. Boyer for their help on the field, and P.-H. Cournède for the use of the Digiplante software (Ecole Centrale Paris, EPI Digiplante).

500

501 **References**

502

503 Barthélémy D. and Caraglio Y., 2007. Plant architecture: a dynamic, multilevel
504 and comprehensive approach to plant form, structure and ontogeny. Ann. Bot.
505 99(3) : 375-407.

506

507 Berg C. C. and Franco Rosselli P., 2005. Cecropia. New York Botanical Garden
508 Press, New York, USA.

509

510 Christophe A., Letort V., Hummel I., Cournede P.-H., de Reffye P. and Lecoeur J.,
511 2008. A model-based analysis of the dynamics of carbon balance at the whole-
512 plant level in Arabidopsis thaliana. Funct. Plant. Biol. 35, 1147–1162.

513

514 Cournède P.-H., Kang M-Z, Mathieu A, Barczi J-F, Yan H-P, Hu B-G and de
515 Reffye P., 2006. Structural factorization of plants to compute their functional and
516 architectural growth. Simulation 82 (7): 427-438.

517

518 Cournède P.-H., Mathieu A., Houllier F., Barthelemy D., and De Reffye P., 2008.
519 Computing Competition for Light in the GREENLAB Model of Plant Growth: A
520 Contribution to the Study of the Effects of Density on Resource Acquisition and
521 Architectural Development,. Ann. Bot. 101(8): 1207-1219.

522

523 Cournède P.-H., Letort V., Mathieu A., Kang M.Z., Lemairee S., Trevezas S.,
524 Houllier F., de Reffye P., 2011. Some Parameter Estimation Issues in Functional-
525 Structural Plant Modelling. Mat. Mod. Nat. Phen., In Press.

526

527 Godin C., Costes E. and Caraglio Y., 1997. Exploring plant topological structure
528 with the amapmod software: an outline. Silva Fennica. 31: 355–366.

529

530 Godin C. and Caraglio Y., 1998. A multiscale model of plant topological
531 structures. J. Theo. Biol. 191: 1–46.

532

533 Guo Y., Ma Y., Zhan Z., Li B., Dingkuhn M., Luquet D. and de ReffyeP ., 2006.
534 Parameter optimization and field validation of the functional-structural model
535 GreenLab for maize. Ann. Bota. 97: 217–230.

536

537 Hallé F., Oldeman R. and Tomlinson P., 1978. Tropical trees and forests, an
538 architectural analysis. Springer-Verlag, New-York.

539

540 Heuret P., Barthélémy D., Guédon Y., Coulmier X. and J. Tancre, 2002.
541 Synchronization of growth, branching and flowering processes in the south
542 american tropical tree Cecropia obtusa (Cecropiaceae). Am. J. Bot.,89(7): 1180–
543 1187.

544

545 Kitajima K., Mulkey S., Samaniego M. and Wright J., 2002. Decline of
546 photosynthetic capacity with leaf age and position in two tropical pioneer species.
547 Am. J. Bot. 89(12): 1925–1932.

548

549 Letort V., Cournède P.-H., Mathieu A., de Reffye P. and Constant T., 2008.
550 Parametric identification of a functional-structural tree growth model and
551 application to beech trees (Fagus sylvatica). Func. Pl. Biol. 35: 951–963.

552

553 Letort V., Heuret P., Zalamea C., Nicolini E. and de Reffye P., 2009. Analysis of
554 Cecropia sciadophylla Morphogenesis Based on a Sink-Source Dynamic Model.
555 In: Li, B.-G. and Jaeger, M. and Guo, Y (eds). 3rd international symposium on
556 Plant Growth and Applications (PMA09), Beijing, China. IEEE Computer
557 Society, pp10-17.

558

559 Lopez G., Favreau R., Smith C., Costes E., Prusinkiewicz P. and DeJong T., 2008.
560 Integrating simulation of architectural development and source-sink behaviour of
561 peach trees by incorporating Markov chains and physiological organ function
562 submodels into L-PEACH. Func. Pl. Biol. 35: 761-771.

563

564 Mathieu A., Cournède P.-H., Letort V., Barthélémy D. and de Reffye P., 2009. A
565 dynamic model of plant growth with interactions between development and

functional mechanisms to study plant structural plasticity related to trophic competition. Ann. Bot. 103: 1173–1186.

Perttunen J., Nikinmaa E., Lechowicz M.J., Sievänen R. and Messier C., 2001. Application of the functional-structural tree model LIGNUM to sugar maple saplings Acer saccharum Marsh) growing in forest gaps. Ann. Bot. 88: 471-481.

Pradal C., Boudon F., Nouguier C., Chopard J. and Godin C., 2009. PlantGL : A python-based geometric library for 3d plant modelling at different scales. Graphical Models. 71: 1–21.

Pretzsch, H., 2002. The single tree-based stand simulator SILVA: construction, application and validation. For. Eco. Man. 162: 3-21.

Prusinkiewicz P., 2004. Modelling plant growth and development. Curr. Op. Pl. Biol. 7: 79–84.

Qi R., Letort V., Kang M.Z., Cournède P-H., de Reffye P. and Fourcaud T., 2009. Application of the GreenLab model to simulate and optimize wood production and tree stability: a theoretical study. Silva Fennica 43(3): 465–487.

R Development Core Team (2008). R: A language and environment for statistical

588 computing. R Foundation for Statistical Computing, Vienna, Austria. ISBN 3-
589 900051-07-0, URL http://www.R-project.org.
590
591 Shinozaki K., Yoda K., Hozumi K. and Kira T., 1964. A quantitative analysis of
592 plant form - the pipe model theory i. basic analysis. Jap. J. Ecol. 14: 97–105.
593
594 Sievänen R., Nikinmaa E., Nygren P., Ozier-Lafontaine H., Perttunen J. and
595 Hakula h., 2000. Components of a functionalstructural tree model. Ann. For. Sci.
596 57: 399–412.
597
598 Yan H.P., Kang M.Z., De Reffye P. and Dingkuhn,M., 2004. A dynamic,
599 architectural plant model simulating resource-dependent growth. Ann. Bot. 93:
600 591-602.
601
602 Yin X., Goudriaan J., Lantinga E.A., Vos J. and Spiertz H.J., 2003. A flexible
603 sigmoid function of determinate growth. Ann. Bot. 91: 361-371
604
605 Zalamea P., Stevenson P., Madrienan S., Aubert P.-M. and Heuret P., 2008.
606 Growth pattern and age determination for Cecropia sciadophylla (Urticaceae).
607 Am. J. Bot. 95: 263–271.
608
609 Zhan Z.G., de Reffye P., Houllier F. and Hu B.G., 2003. Fitting a structural-

functional model with plant architectural data. In: Hu BG, Jaeger M, eds. Proc. Plant Growth Modeling and Applications (PMA03), Beijing, China. Tsinghua University Press and Springer, pp. 236-249.

620 **Tables**

621

622

623

624 Tab. 1. Characteristics of trees measured in September 2007 (ID 1 to 11) and

625 December 2008 (ID 29 to 48).

626

ID	Age	NbPhyts	Loc	H (m)	DBH (cm)	AerMass(kg)	RootMa.(kg)
1	2	55	E	3.61	3.9	5.481	0.96
2	2	55	E	2.97	2.3	1.092	0.216
3	2	45	E	2.2	1.2	0.341	0.054
4	1	18	E	0.35	-	0.038	0.009
5	1	29	E	0.08	-	0.002	0.00047
6	2	33	E	0.71	-	0.07	0.0297
7	2	37	E	0.77	-	0.125	0.044
8	8	248	E	9.87	9.3	40.72	-
9	3	74	E	7.72	9.5	40.605	-
10	8	391	C	12.64	13.4	71.741	-
11	2	52	E	1.49	1.6	0.486	0.083
29	3	86	C	3.87	2.9	1.057	-
30	2	51	C	1.63	1.1	0.179	-
31	2	67	C	2.92	1.91	0.512	-
40	4	99	C	6.16	5.7	4.092	-
41	2	70	C	1.73	1.2	0.193	-
42	2	69	C	2.98	2.44	0.7	-
48	4	74	C	4.8	4.25	2.389	-

627

ID: identifier index, Age: ontogenetical age (years), Nphyt.: total number of

628

phytomers,

629

Loc. : location (E:Saint-Elie, C: Counami), H: height (m), DBH: diameter at

630 breast height (cm),

631 AerMass: total aerial fresh mass (kg), RootMa.: fersh mass of the root system

632 (kg).

633

634

635 Tab. 2. Parameters used in the simulations: parameters for the climate function
636 fitted on St Elie precipitation data, allometries estimated directly from the data,
637 relative local index for each tree (from 1 to 11 for trees of 2007 and from 1 to 7
638 for trees of 2008) and model hidden parameters estimated against the data of
639 2007.

Climate function (temporal variation of the environment)		
A	Amplitude	430.8mm
B	Threshold	74.81mm
m	Month of short dry season	4 (Febr.)
a	Coef. Short dry season	0.446
Allometries estimated directly from data		
r	Biomass proportion to roots	19.00%
Q_0	Initial biomass	0.1g
p_b	Blade sink coefficient	0.7177
p_p	Petiol sink coefficient	0.208
p_i	Internode sink coefficient	0.07423
E^l: Relative local index for each tree		
2007 trees	1.03; 0.81; 0.62; 0.52; 0.33; 0.37; 0.30; 0.98; 1.12; 0.67	
2008 trees	0.50; 0.37; 0.70; 0.70; 0.36; 0.67; 0.83	
Parameters common to all trees		
μ	Production efficiency	$6.4 \cdot 10^{-5}$
P_b	Bud Sink	10 (fixed)
$K_b(1)$	Bud sink param. order 1	0.0062
$K_b(2)$	Bud sink param. order 2	0.0064
P_{fl}	Inflorescence Sink	4.89
T_{fl}	Inflo.expansion duration	7 (fixed)
a_{fl}, b_{fl}	Inflo param. expansion	1.82, 22.8
P_{rg}	Linear sink of rings	0.024
K_{rg}	Q/D-coefficient sink of rings	0.024
SBM_{min}	Initial Specific Blade Mass	0.00749 (fixed)
K_{SBM}	Q/D-coefficient for SBM	0.0012
β	Internode shape coefficient	0.9 (fixed)
Be_{min}	Initial Be (internode shape coef.)	75.1
Be_{max}	Final value of Be	2.66
K_{be}	Q/D-coefficient for Be	0.0069
Ta_{min}	Initial Leaf functioning duration	7 GC (fixed)
K_a	Q/D-coefficient for Ta	1.0

640

641 **Captions of figures**

642

643 Fig. 1. Habit of *Cecropia sciadophylla*. Sequence of internodes of an axis (A),
644 young inflorescence (B), youngest (C) and oldest (D) individuals 4 and 10, that
645 were measured in 2007 (respective heights: 35cm and 12m).

646

647 Fig. 2. Fitting of pluviometry data from St Elie station.

648

649 Fig. 3. Age determination for tree 10. Internode length (bold line) and pith
650 diameter (line) of internodes along the main stem and localization of branches
651 (triangles) and inflorescences (circles).

652

653 Fig. 4. (A) Blade area with respect to fresh petiol section and (B) dry SBM
654 calculated using measured blade area (dark symbols) or blade area that was
655 estimated using the petiol fresh sectional area (open symbols). Gray symbols are
656 plants from the 2008 measurements, for which blade area was not measured.

657

658 Fig. 5. Biomass allocation for primary growth: blade dry mass (A), petiol dry mass
659 (B), and internode dry mass (C) with respect to phytomer dry mass, for each
660 branching order.

661

662 Fig. 6. Measured (dots) and simulated (lines) values of internode mass (a), blade

663 mass (b), petiol mass (c) and inflorescence mass (d) for the main stems of the 11
664 individuals from the data of 2007.
665
666 Fig. 7. Variations of the biomass supply to demand ratio: values at each GC (A)
667 and average values over one year (B) to extract the global trend. Triangles and
668 circles represent the date of appearance of branches and inflorescences. Note: for a
669 better distinction of the curves, Graph A was truncated in its highest values.

Figures

Fig. 1.

678

679

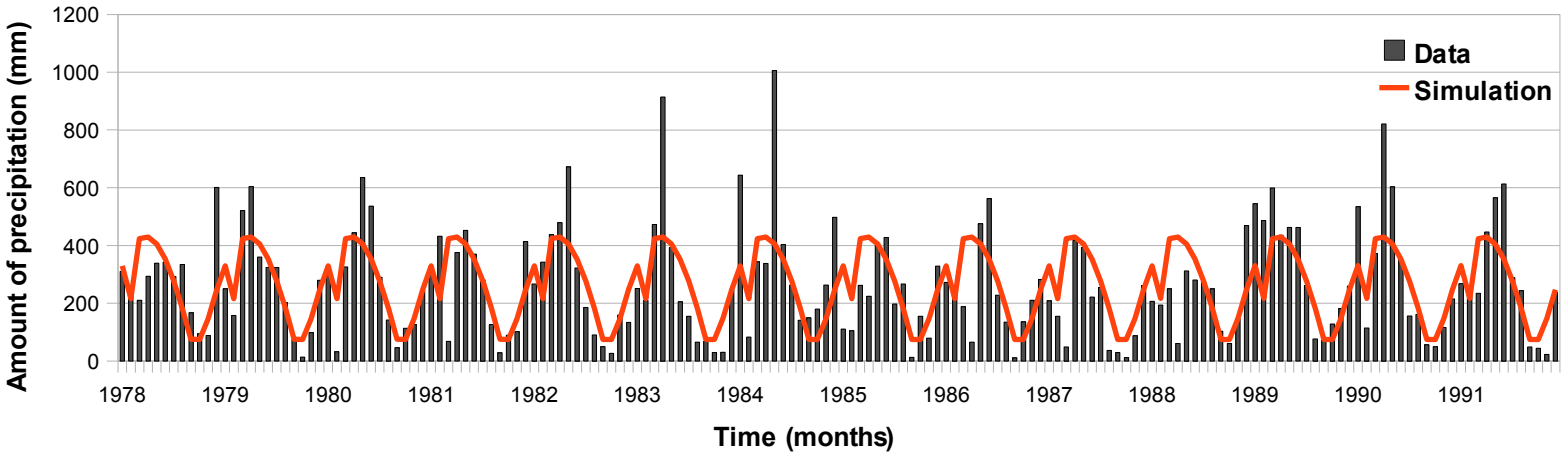

681 Fig. 2.

682

683

684

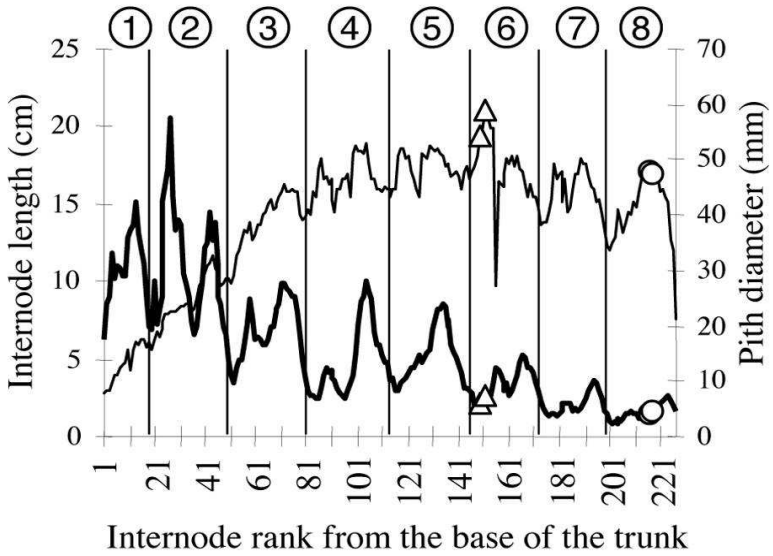

685

686 Fig. 3.

687

688

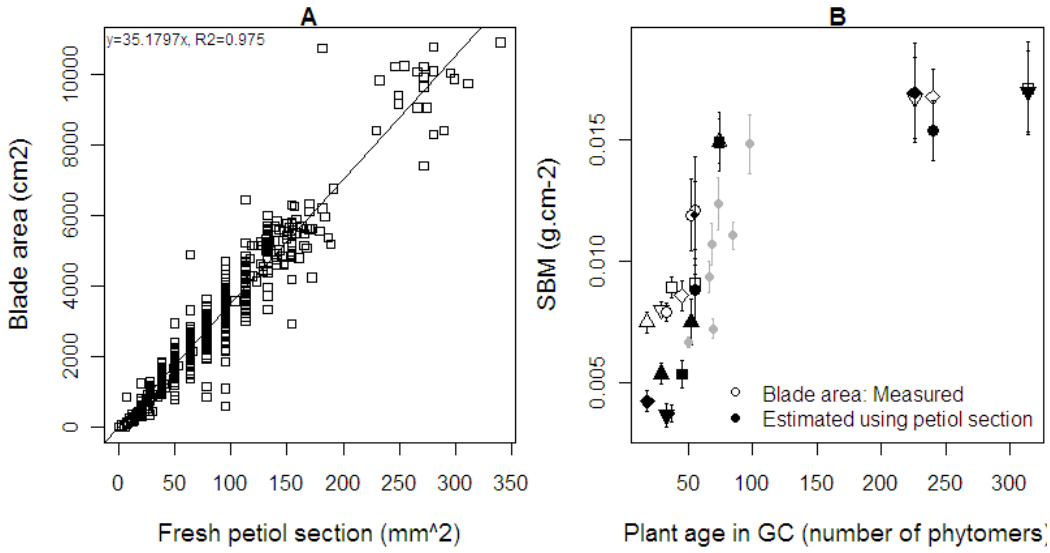

689

690 Fig. 4.

691

692

693

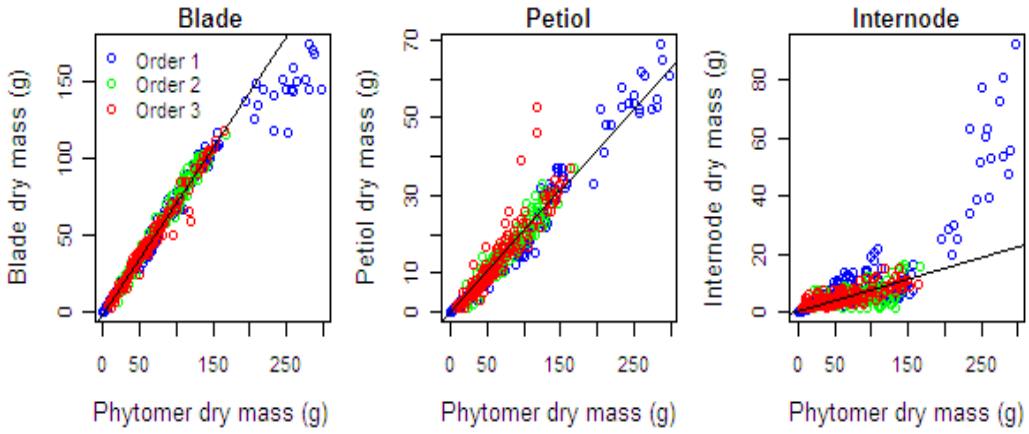

694

695 Fig. 5.

696

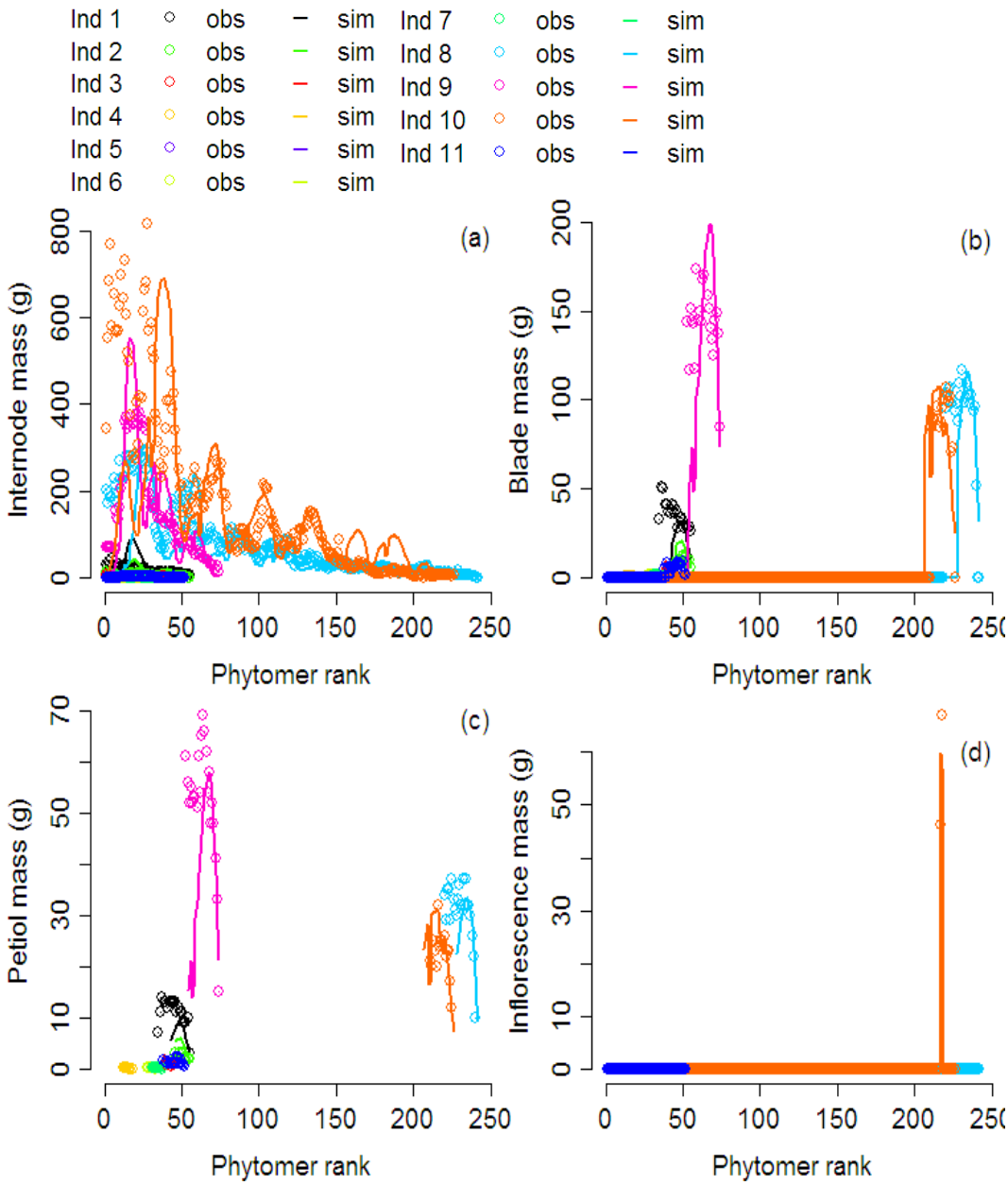

697 Fig. 6.

698

699

700

701

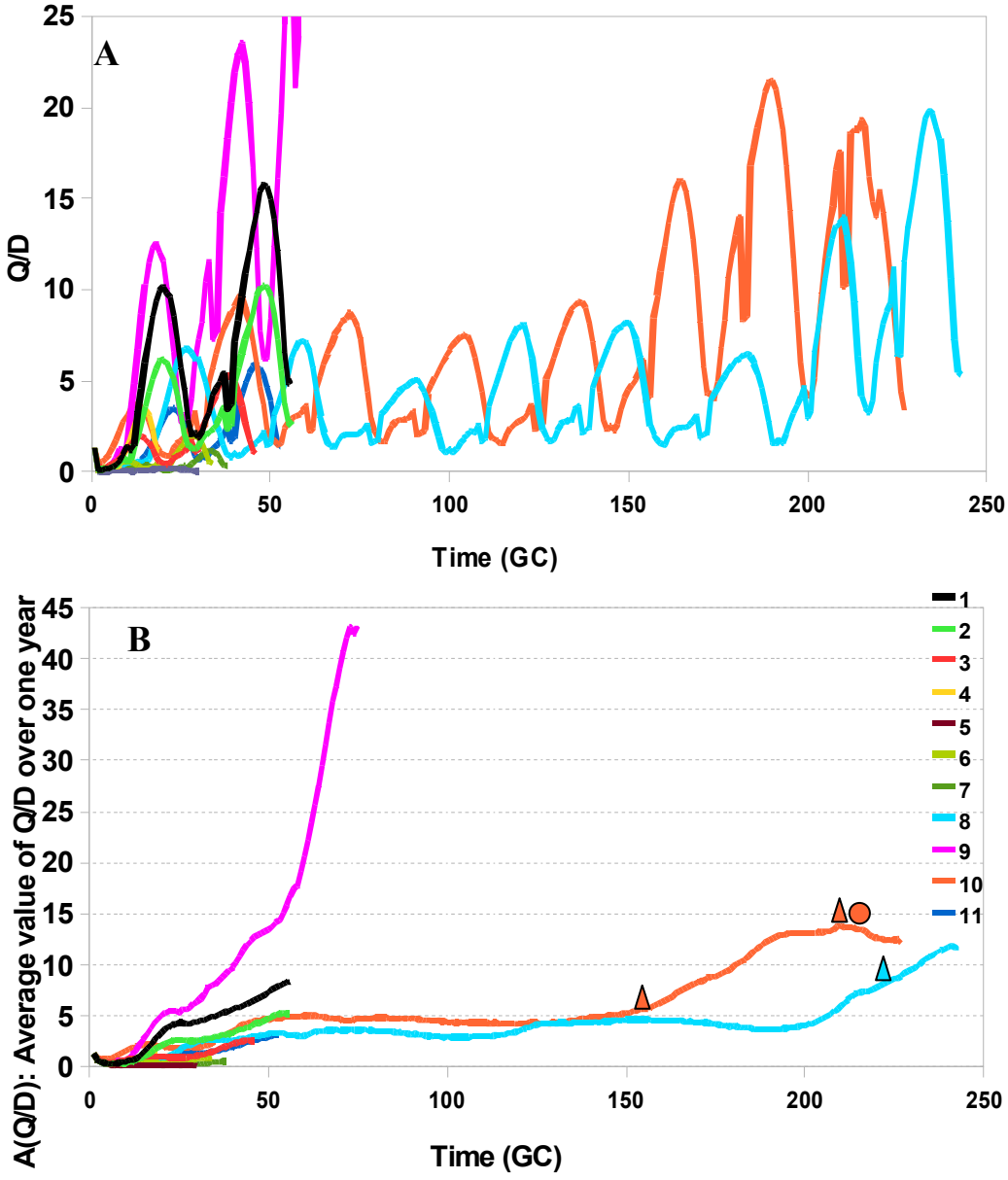

702 Fig. 7.

703